Magnetic Resonance in Medicine 59:190–195 (2008)

# Imaging Cadavers: Cold FLAIR and Noninvasive Brain Thermometry Using CSF Diffusion

Paul S. Tofts,[1*] Jonathan S. Jackson,[1] Daniel J. Tozer,[1] Mara Cercignani,[1] Geoffrey Keir,[1] David G. MacManus,[1] Gerard R. Ridgway,[2] Basil H. Ridha,[1] Klaus Schmierer,[1] Durre Siddique,[1] John S. Thornton,[1] Stephen J. Wroe,[1] and Nick C. Fox[1]

**There is increasing interest in imaging cadavers for noninvasive autopsies for research purposes. However, the temperature is well below that of in vivo imaging, and a variety of interesting 'cold brain' effects are observed. At lower temperatures conventional FLAIR sequences no longer produce dark cerebrospinal fluid (CSF); $T_1$ is reduced from about 4.0 sec in vivo to 1.7 sec at 1°C. The diffusion coefficient (DC) of CSF is much reduced (from 3.1 $10^{-9}$ $m^2s^{-1}$ in vivo to 1.1 at 1°C). DC values therefore provide a noninvasive thermometer to measure brain core temperature to within 1.0°C. In three cadavers DC values were 1.1–1.5 $10^{-9}$ $m^2s^{-1}$, indicating brain core temperatures of 1–10°C, consistent with external thermocouple measurements. An improved inversion time ($TI^0$) can then be found for FLAIR. At 10°C this Cold FLAIR sequence ($TI^0$ = 1.5 sec) gave black CSF. Expressions for CSF DC and $T_1$ as a function of temperature were produced. A measurement of CSF DC could be converted directly to temperature and the required $TI^0$ found. In vitro values of CSF DC were about 1% lower than that of water. Thus, FLAIR imaging can be optimized for cadaveric brains at low and unknown temperatures, thereby improving value for autopsy purposes and facilitating comparisons with in vivo imaging. Magn Reson Med 59:190–195, 2008. © 2007 Wiley-Liss, Inc.**

**Key words: cerebrospinal fluid; diffusion; water; postmortem tissue**

There is increasing interest in MRI of cadavers. Cadaveric imaging involves imaging the intact body after death and the noninvasive nature of cadaveric imaging can be useful to answer specific questions where it is not possible to perform a complete autopsy—for instance, because of lack of consent due to religious, cultural, or ethical reasons (1). In addition, there might be a premium in being able to carry out noninvasive MRI in diseases such as prion disease, where the postmortem material is dangerous to handle. Cadaveric MRI may also provide complementary information to a full conventional autopsy and may, for instance, guide the pathologist to the location of potential histological abnormalities in the brain (2,3). Additionally, if organs such as the brain can be imaged after death without removal from the body, changes and distortions that are the inevitable result of brain removal are avoided. A closer comparison and registration with in vivo imaging is therefore possible with cadaveric imaging than with imaging of the brain after removal. Consequently, it is expected that an improved understanding of the histopathological changes underlying alterations in MR neuroimaging and quantification will facilitate the role of these techniques in clinical diagnosis and disease monitoring.

However, the MRI appearance of the postmortem and cadaver brain, even when normal, is altered in a number of ways. These potentially relate to both changes in the tissue following death and to the fact that usually the tissue is substantially colder than during in vivo imaging (about 37°C), although this is not always the case (4). Excised postmortem tissue, although refrigerated (at about 5°C) during storage, is likely to warm up to room temperature (19–23°C) during imaging unless special precautions are taken. However, a cadaver has a much larger thermal mass and is likely to stay nearer to 5°C during the whole examination. The effect of reduced temperature is generally to reduce $T_1$ and $T_2$ values. In cadavers the effect on cerebrospinal fluid (CSF) is particularly apparent since its relaxation times are so different from parenchymal tissue. (postmortem brain slices usually have empty ventricles when imaged). Other parameters, such as apparent diffusion coefficient (ADC), will also be altered, with CSF again particularly noticeable. Thus, MR imaging sequences that have been optimized for in vivo work do not necessarily perform well in cadavers. In particular, FLAIR imaging (5) is designed to virtually eliminate the CSF signal (in order to increase the conspicuity of periventricular lesions), and the reduction in CSF $T_1$ in cadavers (compared to in vivo) may reduce the effectiveness of the fluid attenuation. It is usually not practicable, in terms of scanning time, to try a range of inversion times to obtain effective fluid attenuation. Thus, there is potential to improve conventional sequences when used for cadaver imaging, and in addition the core temperature of the brain at the time of imaging will not be known.

By taking advantage of the alteration in MR parameters with temperature, a noninvasive in situ thermometer be-

[1]Institute of Neurology, Queen Square, University College London, UK.

[2]Department of Medical Physics and Bioengineering, University College London, UK.

Grant sponsor: Multiple Sclerosis Society of Great Britain and Northern Ireland (to the NMR Research Unit and D.J.T.); Grant sponsor: Brain Research Trust (studentship to J.S.J.); Grant sponsor: Wellcome Trust (to K.S.); Grant sponsor: Alzheimer's Research Trust (to B.G.R.); Grant sponsor: Medical Research Council (UK) Senior Clinical Fellowship (to N.C.F.); Grant sponsors: EPSRC and GlaxoSmithKline (to G.R.R.).

*Current address and correspondence to: Prof Paul Tofts, Brighton and Sussex Medical School, Brighton, BN1 9PS, UK. E-mail: p.s.tofts@bsms.ac.uk

Received 20 February 2007; revised 10 September 2007; accepted 1 October 2007.

DOI 10.1002/mrm.21456

Published online 3 December 2007 in Wiley InterScience (www.interscience.wiley.com).

comes possible. A measurement of $T_1$ or diffusion coefficient (DC) in CSF could provide an estimate of core brain temperature. (The diffusivity in brain tissue is referred to as the ADC since it is apparent and dependent on the diffusion time, because of biological restrictions to diffusion, while in a liquid such as CSF it is a true DC.) CSF $T_1$ and DC decrease by a factor of about 3 between body temperature and 1°C (Figs. 1, 2). Such noninvasive thermometry could have many applications, for example, in situations where invasion of the brain by a conventional thermometer (e.g., mercury in glass) would disrupt tissue structure, or to comply with relatives' wishes that the body be kept intact.

Here we present preliminary measurements of signal intensity and DC values in cold cadavers; we predict how signal intensity will vary with temperature; we propose improved sequence parameters for cadaver FLAIR imaging, and we use DC to estimate the temperature in the brain ventricles of our cadaver. An improved Cold FLAIR sequence is demonstrated, using a reduced inversion time. DC measurements on extracted CSF and water are presented for validation of our technique. The warming rate of the head was estimated to be about 1°C/hr, based on serial measurements of DC. A preliminary account of this work has been presented (6).

## MATERIALS AND METHODS

### Cadaver Imaging

Three cadavers that had previously been refrigerated were imaged. Ethical permission was obtained from the combined Institute and Hospital Ethics Committee and written informed consent to postmortem examination and cadaveric imaging was obtained from each patient's next of kin. Diagnoses, details of estimated times in and since refrigeration, and refrigeration temperatures are all given in Table 1. In cadaver #3 the posterior nasal temperature (nasopharynx) was measured with a thermocouple probe before and after imaging.

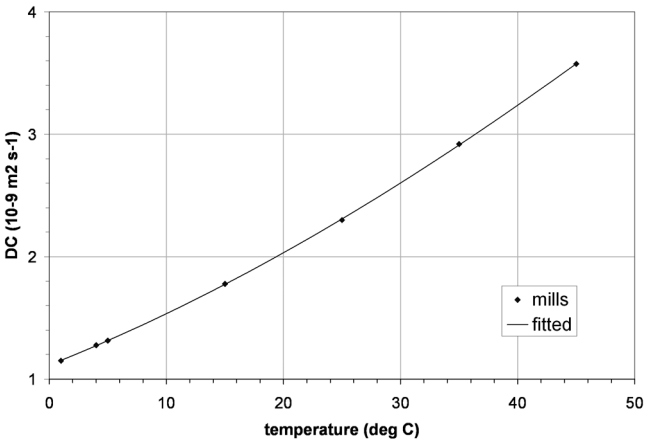


FIG. 1. Water diffusion coefficient (DC) as a function of temperature (fitted to the 1–45°C data of Mills (7), using Eq. [1]). At 37°C the DC is 3.04 $10^{-9}$ $m^2$ $s^{-1}$ (i.e., 3040 $10^{-6}$ $mm^2$ $s^{-1}$), while at 1°C it is down to almost one-third (1.15 $10^{-9}$ $m^2$ $s^{-1}$).

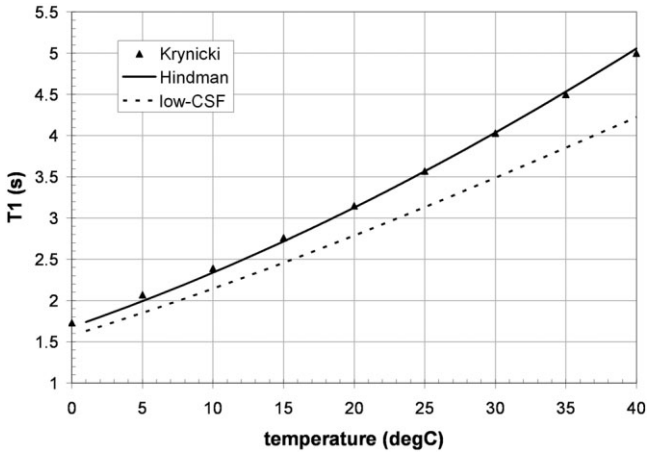


FIG. 2. $T_1$ of pure (deoxygenated) water as a function of temperature (solid line, based on data by Hindman et al. (12), fitted by Eq. [2]). The data of Krynicki (10) are also shown. CSF values could be a little lower (dotted line shown is Eq. [3] with $T_1^{CSF}(37) = 4.0$ sec).

A GE Medical Systems (Milwaukee, WI) 1.5T imager was used with a birdcage transmit-receive head coil. Fast oblique axial FLAIR imaging used TR = 9.9 sec; TE = 166 ms; TI = 2.473 sec; 37 3 mm slices; FOV = 30 × 30 cm; matrix = 320 × 224 (reconstructed to 512 × 512); pixel size = 0.59 × 0.59 mm. In cadavers #2 and #3 additional Cold FLAIR imaging was carried out (TI = 1.5 sec) (see below). Single-shot diffusion-weighted imaging used (nominal) TR = 10 sec; TE = 90 ms; matrix 128 × 128; FOV 24 × 24 cm; 18 axial contiguous slices each 5 mm thick; b = 0, 1000 s $mm^{-2}$ (cadaver #1 had 7 mm slices with a 2 mm gap). Images with the higher b-value were acquired in three orthogonal planes from which an isotropic ADC map was calculated using the manufacturer's commercial software (Functool, GE Medical Systems).

In the cadaver brain the signal intensity of white matter and CSF, the ADC of white matter, and the DC of CSF were measured. For CSF, regions of interest (ROIs) were placed in central portions of ventricles. Adjacent slices were checked to minimize partial volume error. From the CSF DC values, and using Eq. [1] below, the temperature of the CSF was estimated.

### MRI Modeling

To understand the MRI behavior of brain tissues as their temperature is lowered, estimates of tissue parameters (PD, $T_1$, and $T_2$) are required for both CSF and white matter. The DC values of CSF is also of interest since it may constitute a virtual internal thermometer.

The DC of water has been reliably measured by Mills (7) using a diaphragm-cell technique. Reported reproducibility and accuracy for DC values were both about 0.2%; temperature was certain to within 0.01°C. Values (units $10^{-9}$ $m^2$ $s^{-1}$ = 1000 $10^{-6}$ $mm^2$ $s^{-1}$) were 45°C: 3.575; 35°C: 2.919; 25°C: 2.299; 15°C: 1.777; 5°C: 1.313; 4°C: 1.276; 1°C: 1.149. More recent MRI measurements (8) around room temperature are in agreement (25°C: 2.315; 95% confidence interval [CI]: 2.280–2.350).

Table 1
Details of Three Cadavers Imaged

| Cadaver # | diagnosis | Duration of refrigeration (hr) | Warming time (hr) | CSF DC $10^{-9}$ m$^2$ s$^{-1}$ (±95%CI) | Estimated brain core temperature °C (±95% CI) | FLAIR signal ratio CSF/WM | |
|---|---|---|---|---|---|---|---|
| | | | | | | TI = 2.47 | T I =1.5 sec |
| 1 | CJD | 48[a] | 1 | 1.15 (±0.03) | 1.0 (±0.8) | 4.12 | — |
| 2 | FTD[b] | 18 | 2 | 1.52[c] (±0.01) | 9.7 (±0.2)[d] | 4.11 | 0.17 |
| 3 | FTD | 14 | 2 | 1.53[c] (±0.01) | 9.9 (±0.2)[e] | 2.95 | 0.26 |

[a]For this case, the refrigerator temperature control was known to be unreliable.
[b]FTD = frontotemporal dementia.
[c]The improved slice center separation (5 mm vs. 9 mm for cadaver #1) reduced partial volume effects and gave an improved 95% CI.
[d]A 2nd measurement, 1.5 hr later, gave 11.2°C, and hence a warming rate of 1.1°C/h.
[e]A 2nd measurement, 1.5 hr later, gave 12.0°C, and hence a warming rate of 1.3°C/h. The posterior nasal temperature, measured with a thermocouple probe, was 11°C before imaging, and 16°C 2 hr later.

The water DC data at six discrete temperatures from Mills were interpolated to provide water DC as a continuous function of temperature D(T) (T in °C) as follows. An Arrhenius plot (7) of $\log_{10}$(D) vs. 1/(absolute temperature) fitted the data quite well (absolute temperature = T + $T_0$; $T_0$ = 273.15 K), with a maximum residual of 2.0%. Inspection of the residuals showed a parabolic behavior. Adding a quadratic term to the Arrhenius expression, centered around a reference temperature $T_R$ near the center of the required temperature range, has worked well for other DC data (8); this Taylor expansion term gives a small correction to the linear expression, improving accuracy and allowing the expression to work over a wider range of temperature:

$$\log_{10}D(T) = A + B\left(\frac{1}{T+T_0} - \frac{1}{T_R+T_0}\right) + C\left(\frac{1}{T+T_0} - \frac{1}{T_R+T_0}\right)^2 \quad [1]$$

Using this expression, the Mills data were well represented (Fig. 1), with a maximum residual of 0.41% (rms residual 0.25%). Fitted values ($T_R$ = 15°C) were A = 0.24882, B = −1013.1, C = −25,150. Fitting was carried out using a Microsoft Excel spreadsheet; conditioning was improved by scaling the three free parameters to be near to unity. Note that by fitting log(D), (not D), the fractional residuals (not the absolute residuals), are minimized. At body temperature (37°C) water DC is 3.04 $10^{-9}$ m$^2$ s$^{-1}$ (i.e., 3040 $10^{-6}$ mm$^2$ s$^{-1}$).

The $T_1$ of water as a function of temperature has been well documented by Krynicki (9), Tofts (10), and Hindman et al. (11), and these values were used to simulate the signal of CSF. Earlier results (13) showed more variation. Krynicki used a CW saturation recovery technique at 28 MHz and presented interpolated data (95% CI = ±3%). Hindman et al. used an inversion recovery pulse sequence at 60 MHz (95% CI = ±2%). Since the $T_1$ of water is independent of field strength (caused by the extreme motional narrowing (13)), these values can in principle be used for any field strength. Both datasets could be well fitted by a quadratic Arrhenius expression (see Eq. [1]). There were no signs of any systematic deviation of the model from the data. The fitted expressions for each dataset agreed well over most of the temperature range. At the extremes, systematic differences were apparent; at 1°C the Krynicki data were 60 ms higher than the Hindman et al. data, and at 37°C they were 45 ms lower. The Hindman et al. data were chosen as more appropriate on the basis of the methodology. These are fitted by:

$$\log_{10}T_1(T) = A + B\left(\frac{1}{T+T_0} - \frac{1}{T_R+T_0}\right) + C\left(\frac{1}{T+T_0} - \frac{1}{T_R+T_0}\right)^2 \quad [2]$$

with a maximum residual of 2.2% (rms residual 0.8%). Fitted parameter values ($T_R$ = 20°C; $T_0$ = 273.15K) were A = 0.49512, B = −1015.2, C = −263,170. Spot fitted values for $T_1$ were: 1°C: 1.739s; 23°C: 3.388s; 37°C: 4.740 sec (see Fig. 2).

The $T_1$ of CSF was modeled, as a function of temperature, by starting with the value for water and then reducing it slightly by adding a small fixed amount to the relaxation rate ($R_1 = 1/T_1$) to account for the possible effects of dissolved oxygen:

$$\frac{1}{T_1^{CSF}(T)} = \frac{1}{T_1^{water}(T)} + \left(\frac{1}{T_1^{CSF}(37)} - \frac{1}{T_1^{water}(37)}\right) \quad [3]$$

Thus, at 37°C $T_1^{water}$ = 4.74 sec, and $T_1^{CSF}$ values in the range 4.0−4.7 sec were used (Fig. 2).

The signals S from CSF and white matter were predicted as a function of temperature using a standard expression for the FLAIR inversion recovery sequence:

$$S_{FLAIR} = PD(1 - 2e^{-TI/T_1} + e^{-TR/T_1})e^{-TE/T_2} \quad [4]$$

The TI value required to produce a FLAIR signal null in CSF was predicted as a function of $T_1$, and hence temperature, from:

$$TI^0 = T_1 \ln\left(\frac{2}{1+e^{-TR/T_1}}\right) \quad [5]$$

(This equation is derived from Eq. [4] and $T_1$ is given by Eq. [2].)

In some situations it may be possible to calculate DC values on the imager at the time of data collection. In this case an immediate estimate of $TI^0$ would be useful. A direct relationship from measured DC to $TI^0$ was made as follows. For a given DC, Eq [1] was solved numerically to give T. From this, $T_1$ and hence $TI^0$ were obtained from Eqs. [2, 5].

### In Vitro DC Measurements on Water and CSF

A multishot EPI sequence for measuring DC in small liquid samples was developed with the aim of looking for any systematic differences between CSF and water. Imaging parameters were: TE = 59 ms, TR = 3 sec, b = 0.700 s $mm^{-2}$, six directions of gradient, echo-train length = 2, pixel size 2.2 × 2.2 mm, slice thickness 3 mm, image matrix 64 × 64. Conventional single-shot EPI-based techniques, developed for use in brain, produce unacceptable susceptibility artifacts with isolated samples that are surrounded by air. Samples were in tubes (internal diameter 20 mm, length 80 mm). Elliptical ROIs (area 230–250 $mm^2$) were placed to avoid edge artifacts. Four samples were measured at a range of temperatures: water, CSF1, CSF2, and CSF(Hb), which had some blood breakdown products in it. The CSF samples had been frozen, defrosted, and then refrigerated for 2 weeks, with sodium azide added as a preservative.

## RESULTS

### Cadaver Imaging

The measured DC values of CSF ranged from 1.1–1.5 $10^{-9}$ $m^2$ $s^{-1}$ (1100–1500 $10^{-6}$ $mm^2$ $s^{-1}$) (see Table 1). Normal-appearing white matter ADC values were 0.14 $10^{-9}$ $m^2$ $s^{-1}$ (cadaver #1), 0.19 $10^{-9}$ $m^2$ $s^{-1}$ (cadaver #2), 0.18 $10^{-9}$ $m^2$ $s^{-1}$ (cadaver #3). Corresponding brain core temperatures were 1–10°C. In cadaver #3 the posterior nasal temperature was 11°C before imaging and 16°C after imaging.

The CSF signal in FLAIR images was noticeably brighter than in in vivo images. With conventional FLAIR, CSF/WM signal ratios were in the range 3.0–4.1 (Table 1); Cold FLAIR reduced this very effectively (ratios of 0.2–0.3, see Table 1, Fig. 3).

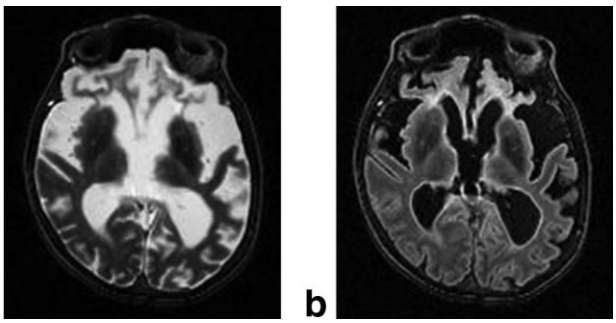


FIG. 3. Conventional and Cold FLAIR images, from cadaver #2. **a:** TI = 2.473 sec. **b:** TI = 1.5 sec. Brain temperature = 10°C. Cold FLAIR eliminates CSF flare.

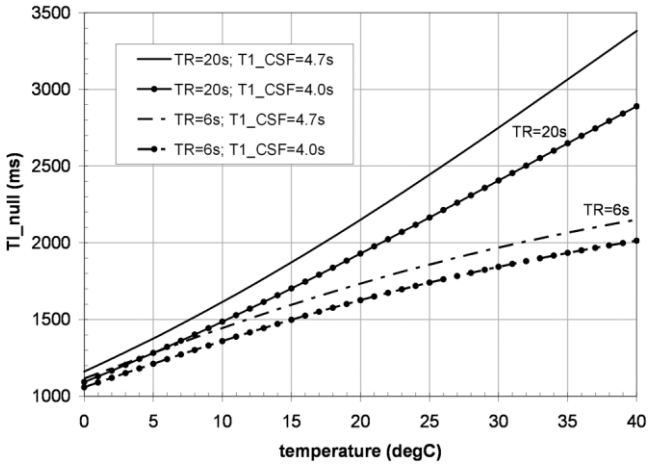


FIG. 4. Predicted inversion times $TI^0$ to null CSF in a FLAIR sequence (from Eq. [6]). Values are shown for a range of typical TR values (6–20 sec); more TR values are accommodated in Table 2. The spread due to uncertainty in the $T_1$ of CSF is shown. T1_CSF values in the legend refer to 37°C; the upper and lower confidence limits in normal CSF are 4.0 and 4.7 sec.

### MRI Modeling

The simulations confirmed an increase in CSF signal as temperature is reduced.

FLAIR null times (from Eq. [5]) predicted $TI^0$ at room temperature to be 1.7–2.3 sec (for TR in the range 6–20 sec), reducing to 1.1–1.2 sec at 1°C (Fig. 4). A general purpose Cold FLAIR value of $TI^0$ = 1.5 sec was chosen for imaging cadavers #2 and #3.

The relationship between the measured CSF diffusion coefficient value and inversion time $TI^0$ required for FLAIR nulling is shown in Table 2.

### In Vitro DC Measurements on Water and CSF

Measured DC values of water were 2–3% higher than those of Mills (using Eq. [1]) (Fig. 5). The CSF(Hb) sample was not significantly different from the other two CSF samples. Pooled values for CSF (three samples, four temperatures) had a significantly lower DC than water (difference −0.013 $10^{-9}$ $m^2$ $s^{-1}$; 95% CI 0.011–0.015), although this only represents about 1% of the absolute DC. The water bath warmed by no more than 0.35°C during the period of imaging.

## DISCUSSION

The DC of CSF has been measured in vivo by two groups. Annet et al. (14) found a range of 2.98–3.37 $10^{-9}$ $m^2$ $s^{-1}$ in six subjects (mean = 3.18). Hakyemez et al. (15) found a range of 3.21–3.76 $10^{-9}$ $m^2$ $s^{-1}$ in 15 subjects (mean = 3.42). A third group (16) estimated a value of 3.0. The measured DC of CSF could be artificially higher than the DC of water at the same temperature (if there was a contribution from CSF pulsation artifact), or it could be lower (if there was a partial volume error with surrounding white matter, or if there was suspended cellular debris in the ventricles). Given that one published dataset range in-

Table 2
Look-up Table to Convert from Measured CSF Diffusion Coefficient (DC) to Temperature and Hence Cold FLAIR $TI^0$ Value

| CSF DC ($10^{-9}$ $m^2$ $s^{-1}$) | Temperature[a] (°C) | $T_1^{CSF}$ [b] (s) | $TI^0$ [c] | | | |
|---|---|---|---|---|---|---|
| | | | TR = 4 sec | TR = 6 sec | TR = 10 sec | TR = 20 sec |
| 1.1 | -0.4 | 1.60 | 0.98 | 1.07 | 1.11 | 1.11 |
| 1.2 | 2.2 | 1.75 | 1.04 | 1.16 | 1.20 | 1.21 |
| 1.3 | 4.7 | 1.89 | 1.10 | 1.23 | 1.30 | 1.31 |
| 1.4 | 7.0 | 2.03 | 1.14 | 1.31 | 1.40 | 1.41 |
| 1.5 | 9.3 | 2.18 | 1.19 | 1.38 | 1.49 | 1.51 |
| 1.6 | 11.4 | 2.32 | 1.23 | 1.44 | 1.58 | 1.61 |
| 1.7 | 13.5 | 2.46 | 1.26 | 1.50 | 1.66 | 1.71 |
| 1.8 | 15.5 | 2.60 | 1.30 | 1.56 | 1.75 | 1.80 |
| 1.8 | 17.5 | 2.75 | 1.33 | 1.61 | 1.83 | 1.90 |
| 2.0 | 19.4 | 2.88 | 1.36 | 1.66 | 1.91 | 2.00 |
| 2.1 | 21.3 | 3.02 | 1.38 | 1.71 | 1.99 | 2.09 |
| 2.2 | 23.1 | 3.16 | 1.41 | 1.75 | 2.06 | 2.19 |
| 2.3 | 24.8 | 3.30 | 1.43 | 1.79 | 2.13 | 2.28 |
| 2.4 | 26.6 | 3.44 | 1.45 | 1.83 | 2.20 | 2.37 |
| 2.5 | 28.3 | 3.56 | 1.47 | 1.87 | 2.27 | 2.46 |
| 2.6 | 30.0 | 3.71 | 1.49 | 1.90 | 2.33 | 2.55 |
| 2.7 | 31.6 | 3.85 | 1.50 | 1.93 | 2.39 | 2.64 |
| 2.8 | 33.2 | 3.98 | 1.52 | 1.96 | 2.45 | 2.73 |
| 2.9 | 34.9 | 4.11 | 1.53 | 1.99 | 2.50 | 2.82 |
| 3.0 | 36.4 | 4.25 | 1.55 | 2.02 | 2.56 | 2.91 |
| 3.1 | 37.9 | 4.38 | 1.56 | 2.04 | 2.61 | 2.99 |

[a]From Eq. [1].
[b]From Eqs. [2,3], assuming $T_1^{CSF}(37) = 4.3$ sec.
[c]From Eq. [5].

cludes the DC of water, while the other is higher than that of water, we concluded that the DC of normal CSF is not reduced substantially below that of water by the presence of debris, and that the best estimate for CSF DC is to use the DC of water. In vitro measurements of the DC of water and CSF were made to confirm this (see Fig. 5).

Noninvasive brain core thermometry using the CSF DC does seem to be reliable. Although in principle the DC might be vulnerable to presence of suspended cellular debris in the ventricles (possibly increased in the presence of parenchymal pathology), which could reduce its value, the evidence suggests that this is a small effect (about 1% reduction in DC; see Fig. 5). In a cadaver any debris might be expected to settle to the bottom of the ventricle. Other systematic errors could originate from either the water DC value being used (i.e., Eq. [1], which could be up to 0.6% in error), or from the particular MRI sequence being used (which can be checked using regular water QA at a known temperature). Random error is less than 0.3°C (Table 1), and overall uncertainty is less than 1°C. This is the first publication of precise measurements of the DC of CSF, and for the first time a systematic (though small) reduction in values below that of water has been observed.

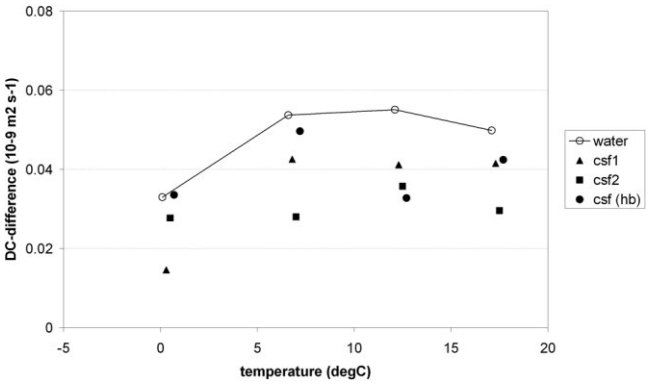


FIG. 5. In vitro measurements of DC in water and CSF. The difference between the measured values and those of Mills (represented by Fig. 1 and Eq. [1]) is shown. For reference, the Mills value for water at 5°C is 1.313 $10^{-9}$ $m^2$ $s^{-1}$. CSF has a slightly lower DC than water (the mean difference is $-0.013$ $10^{-9}$ $m^2$ $s^{-1}$).

The DC values in CSF (Fig. 5) indicate that the DC of CSF is about 1% lower than that of water. This is consistent with the presence of small amounts of dissolved protein, which increase the viscosity slightly. By ignoring this, and using the DC of water for thermometry, there is a systematic error in temperature measurements of about 0.3°C; this is less important than the systematic error in the water DC measurements, which is on the order of 2–3% (i.e., 1°C).

The warming rate that we observed (Table 1) is consistent with that observed in a realistic thermal head phantom (a honeydew melon, mass 1.55 kg, size 16 × 14 × 14 cm), where core temperature rose linearly at 1.8°C $h^{-1}$.

The $T_1$ of CSF is very dependent on oxygen content (17); at 0.15T and 37°C it decreased by 573 ms after equilibration with air. Moreover, its measurement is often inaccurate because $B_1$ errors can result in imperfect inversion. The $T_1$ of CSF in vivo has been measured by Hopkins et al. (18). The mean value was 4.3 sec (range 4.22–4.36 at three fields 0.15–1.4T), estimated inaccuracy <10%. Water measurements at room temperature gave 3.5 sec (the value found by others (9,11) at 24°C; Fig. 2), suggesting that their technique was good. The CSF value is just below that of water at 37°C (4.7 sec); this possible small difference was

ascribed to the effects of dissolved paramagnetic oxygen and possibly cellular debris and blood products. More recently, Zaharchuk et al. (19) measured $T_1$ = 4.09 sec in vivo at 1.5T (estimated 95% CI = ±0.16 sec), and demonstrated the dependence on $pO_2$.

Our attempts to use other MR parameters ($T_1$ and spectroscopy) as virtual thermometers were unsuccessful. Estimated $T_1$ values are dependent on oxygen content and flip angle accuracy. Although the separation between the water and N-acetyl aspartate (NAA) spectroscopic peaks has been used to measure temperature, in our studies the NAA peak was reduced, broadened, and distorted. In spin-echo imaging, attempts to reduce CSF signal down to that of white matter were also unsuccessful (as the tissue cools the $T_1$ values of CSF and white matter become closer).

The Cold FLAIR sequence, with its reduced TI, is completely able to suppress CSF flare (Fig. 3). This TI reduction will also alter image contrast in the parenchyma; in particular, any long-$T_1$ lesions will tend to be darkened. Complete nulling, as suggested in Table 2, will require an accurate 180° inversion pulse (which may be compromised by $B_1$ errors). The CSF $T_1$ values we used to calculate $TI^0$ may be slightly in error (by no more than 10%). In addition, the fast FLAIR sequence is only approximately described by Eq. [4]. Thus, small adjustments to TI might be necessary for complete nulling.

A previous postmortem report (2) using a conventional TI value had shown poor FLAIR contrast, ascribed to blood and protein in the CSF reducing $T_1$. Our results suggest that the high FLAIR signal was in fact caused by the brain being cold.

Our results in Table 2, where CSF DC is used to estimate temperature and FLAIR $TI^0$ values, show that a simple procedure for obtaining CSF nulling is possible. This is likely to be independent of field strength, and therefore applicable at 3T, since for water both $T_1$ and DC are field-independent.

## CONCLUSIONS

1. DC and $T_1$ values for CSF are close to those of pure water (Figs. 1, 2). Reliable water values are available in the literature. CSF $T_1$ values may be reduced a little below those of water by dissolved $O_2$ and cellular impurities. CSF DC values are about 1% below those of water (Fig. 5).
2. CSF DC thermometry is reliable to within <1°C. It has potential for noninvasive measurement, particularly when invasion is prohibited (Table 1).
3. CSF suppression in cold brains is possible with reduced inversion time TI (Table 2, Fig. 4); CSF flare was removed with Cold FLAIR (Fig. 3).
4. Cadaveric imaging may be improved using optimized sequences based on noninvasive determination of the temperature of the tissues to be imaged; this may have implications for studies assessing the utility of noninvasive (MRI) autopsies and for research studies seeking to compare cadaveric imaging with premortem imaging and/or postmortem histology.

## ACKNOWLEDGMENT

We thank Harpreet Hyare for clinical care.

## REFERENCES

1. Griffiths PD, Paley MN, Whitby EH. Post-mortem MRI as an adjunct to fetal or neonatal autopsy. Lancet 2005;365:1271–1273.
2. Geurts JJ, Bo L, Pouwels PJ, Castelijns JA, Polman CH, Barkhof F. Cortical lesions in multiple sclerosis: combined postmortem MR imaging and histopathology. AJNR Am J Neuroradiol 2005;26:572–577.
3. Schmierer K, Scaravilli F, Altmann DR, Barker GJ, Miller DH. Magnetization transfer ratio and myelin in postmortem multiple sclerosis brain. Ann Neurol 2004;56:407–415.
4. Mottershead JP, Schmierer K, Clemence M, Thornton JS, Scaravilli F, Barker GJ, Tofts PS, Newcombe J, Cuzner ML, Ordidge RJ, McDonald WI, Miller DH. High field MRI correlates of myelin content and axonal density in multiple sclerosis—a post-mortem study of the spinal cord. J Neurol 2003;250:1293–1301.
5. Hajnal JV, Bryant DJ, Kasuboski L, Pattany PM, De CB, Lewis PD, Pennock JM, Oatridge A, Young IR, Bydder GM. Use of fluid attenuated inversion recovery (FLAIR) pulse sequences in MRI of the brain. J Comput Assist Tomogr 1992;16:841–844.
6. Tofts PS, Tozer DJ, MacManus DG, Schmierer K, Fox NC. Imaging cadavers — 'cold brain' MRI effects and noninvasive diffusion thermometry of the CSF. IN: Proc 14th Annual Meeting ISMRM, Seattle. 2006; p 2096.
7. Mills R. Self-diffusion in normal and heavy water in the range 1-45°. J Phys Chem 1973;77:685–688.
8. Tofts PS, Lloyd D, Clark CA, Barker GJ, Parker GJ, McConville P, Baldock C, Pope JM. Test liquids for quantitative MRI measurements of self-diffusion coefficient in vivo. Magn Reson Med 2000;43:368–374.
9. Krynicki K. Proton spin lattice relaxation in pure water between 0°C and 100°C. Physica 1966;32:167–178.
10. Tofts PS. QA: quality assurance, accuracy, precision and phantoms. In: Tofts P, editor. Quantitative MRI of the brain: measuring changes caused by disease. Chichester, UK: John Wiley & Sons. 2003; p 55–81.
11. Hindman JC, Svirmickas A, Wood M. Relaxation processes in water. A study of the proton spin-lattice relaxation time. J Chem Phys 1973;59: 1517–1522.
12. Simpson JH, Carr HY. Diffusion and nuclear spin relaxation in water. Phys Rev 1958;111:1201–1202.
13. Callaghan PT. Principles of nuclear magnetic resonance microscopy. Oxford: Clarendon Press; 1991.
14. Annet L, Duprez T, Grandin C, Dooms G, Collard A, Cosnard G. Apparent diffusion coefficient measurements within intracranial epidermoid cysts in six patients. Neuroradiology 2002;44:326–328.
15. Hakyemez B, Aksoy U, Yildiz H, Ergin N. Intracranial epidermoid cysts: diffusion-weighted, FLAIR and conventional MR findings. Eur J Radiol 2005;54:214–220.
16. Latour LL, Warach S. Cerebral spinal fluid contamination of the measurement of the apparent diffusion coefficient of water in acute stroke. Magn Reson Med 2002;48:478–486.
17. Grant R, Condon B, Moyns S, Patterson J, Hadley D, Teasdale G. Temporal physiochemical changes during in vitro relaxation time measurements: the cerebrospinal fluid. Magn Reson Med 1988;6:397–402.
18. Hopkins AL, Yeung HN, Bratton CB. Multiple field strength in vivo T1 and T2 for cerebrospinal fluid protons. Magn Reson Med 1986;3:303–311.
19. Zaharchuk G, Martin AJ, Rosenthal G, Manley GT, Dillon WP. Measurement of cerebrospinal fluid oxygen partial pressure in humans using MRI. Magn Reson Med 2005;54:113–121.